PERMAFROST AND PERIGLACIAL PROCESSES
Permafrost and Periglac. Process. **25**: 295–306 (2014)
Published online 20 November 2014 in Wiley Online Library
(wileyonlinelibrary.com) DOI: 10.1002/ppp.1824

Temperature Regimes of the Active Layer and Seasonally Frozen Ground under a Forest-Steppe Mosaic, Mongolia

Avirmed Dashtseren,[1]* *Mamoru Ishikawa,*[1] *Yoshihiro Iijima*[2] *and Yamkin Jambaljav*[3]

[1] Graduate School of Environmental Science, Hokkaido University, Sapporo, Hokkaido, Japan
[2] Research and Development Center for Global Change, Japan Agency for Marine-Earth Science and Technology, Yokosuka, Japan
[3] Institute of Geography, Mongolian Academy of Science, Ulaanbaatar, Mongolia

ABSTRACT

Permafrost underlying forested north-facing slopes and seasonally frozen ground underlying mountain steppes on south-facing slopes co-exist within a small mountain basin that represents the most general landscape type in northern central Mongolia. A 5-year time series of hydro-meteorological parameters on these slopes is presented in order to identify the factors controlling ground temperature regimes. A thick organic layer (0.2–0.4 m) beneath the forest on a north-facing slope impedes the effects of summer air temperature on the ground, and the forest canopy strongly blocks downward shortwave radiation during summer. Active layer thickness was determined by summer warmth. The mountain steppe on a dry south-facing slope receives a large amount of downward shortwave radiation compared to an adjacent forested slope, and therefore the surface temperature exceeds air temperature during summer, leading to a warm soil profile. In winter, snow cover was the main factor controlling interannual variations in the thickness of seasonally frozen ground. The onset of soil thawing in the forested area was later than in the mountain steppe, even though soil freezing began simultaneously in both areas. Overall, the forest cover keeps the ground cool and allows permafrost to persist in this region. Copyright © 2014 John Wiley & Sons, Ltd.

KEY WORDS: active layer; seasonal frozen ground; forest-steppe; local climate parameters; Mongolia

INTRODUCTION

In recent decades, many regions in the northern hemisphere have witnessed increases in the thickness of the active layer and decreases in the thickness of seasonally frozen ground as a result of climate change (Frauenfeld *et al*., 2004; Zhang *et al*., 2005; Sharkhuu *et al*., 2007; Wu and Zhang, 2010; Zhao *et al*., 2010; Frauenfeld and Zhang, 2011). As heat and energy exchanges occur through these layers, such changes have the potential to alter the surface energy balance, hydrologic cycle, carbon fluxes and ecosystem performance (Brown *et al*., 2000). Therefore, it is important to understand the thermal regimes controlling the development of the active layer and seasonally frozen ground, despite these being complexly determined by factors such as surface temperature, snow cover, land cover, subsurface materials and soil moisture (Brown *et al*., 2000; Walker *et al*., 2003; Zhang, 2005; Ishikawa *et al*., 2006; Iijima *et al*., 2010; Shiklomanov *et al*., 2010).

The type of vegetation cover changes from a Siberian boreal forest region in northern Mongolia to wide steppe in central Mongolia, and this transition corresponds roughly to a change from the Siberian discontinuous permafrost zone to the sporadic permafrost zone. Although steppe is one of the largest natural zones in the country (Batima and Dagvadorj, 2000), forested regions cover 8.1 per cent of the total land area in Mongolia, and are composed mainly of the larch species *Larix sibirica* (Tsogtbaatar, 2004). The permafrost distribution is mosaic-like because Mongolia is located at the southern boundary of the Siberian permafrost, and the thickness of the active layer and seasonally frozen ground show large spatial variations. Such variations depend on the microclimate associated with the topography, thermal properties of the soils and the vegetation cover on a local scale. Country-wide observations have indicated that permafrost temperatures vary with not only latitude, reflecting the meso-scale climatic setting, but also with local factors such as solar radiation, the wetness index and tree shading (Etzelmüller *et al*., 2006; Heggem *et al*., 2006;

*Correspondence to: D. Avirmed, Graduate School of Environmental Science, Hokkaido University, Kita 8, Nishi 5, Kita-ku, Sapporo, Hokkaido 060-0808, Japan.
E-mail: dashka.ig@gmail.com

Received 14 February 2014
Revised 12 September 2014
Accepted 5 October 2014

Sharkhuu *et al*., 2007; Zhao *et al*., 2010; Ishikawa *et al*., 2012; Wu *et al*., 2012).

In Mongolia, permafrost directly sustains the livelihoods of inhabitants because it produces locally wet soil conditions, even under a low annual rainfall of only 50–500 mm . Furthermore, the forests are distributed in a mosaic pattern and overlap considerably with permafrost regions (Ishikawa *et al*., 2005), and river discharges originate entirely from the high mountains and northern territory where permafrost occurs extensively. Further projected climate warming (Batima, 2006) may degrade the permafrost and decrease the productivity of Siberian larch (Dulamsuren *et al*., 2011) and it is therefore crucial to understand the physical interactions between ground temperature, vegetation cover and the atmospheric conditions in such a mosaic region.

Since 2003, hydro-meteorological components have been continuously measured at sites in northern Mongolia, with the goal of delineating the different hydrological characteristics of the mountain steppe on south-facing slopes and those of the forest on north-facing slopes (Ishikawa *et al*., 2005; Iijima *et al*., 2012). Permafrost in the region develops only under forested north-facing slopes (Ishikawa *et al*., 2005), and has an important role in sustaining local river water resources (Iijima *et al*., 2012). The purpose of this paper is to describe 5-year records of comparable hydro-meteorological parameters on these slopes, with particular focus on the distinctive features controlling the ground temperature regimes of the active layer and seasonally frozen ground on these contrasting slopes.

STUDY AREA AND METHODS

Site Distribution

The observation sites are located in the basin of the Shiljiree River, a tributary of the Tuul River in the Khentii Range, north central Mongolia, a mountainous area within the discontinuous permafrost zone (Figure 1). The elevation of the basin ranges from 1550 m asl in the river valley to 2195 m asl on the mountain top. Siberian boreal forest (*L. sibirica* Ledeb and *Pinus*) is predominant on north-facing slopes (Sugita *et al*., 2007; Dulamsuren *et al*., 2011) where permafrost is found (Ishikawa *et al*., 2005, 2008), and mountain steppe is predominant on south-facing slopes where there is no permafrost (Ishikawa *et al*., 2005, 2008). The soil texture of the north-facing slopes is complex; the upper surface layer contains humus and moss, and the lower layers contain silt, sand and gravel. The thickness of the organic layer on these forested slopes ranges from 0.2 to 0.4 m. In contrast, the south-facing slopes are underlain by a thin organic layer measuring up to 0.05 m thick, and the lower part of the soil is composed of sandy gravels (Ishikawa *et al*., 2005).

Automatic soil weather stations, including sensors of ground temperatures and moisture in boreholes, were installed at sites SS and FN, about 1.58 km apart and with slope inclinations of 11–12° (Figure 1). Site SS is on a south-facing slope (1662 m asl) covered by mountain steppe, on seasonally frozen ground. Site FN is on a

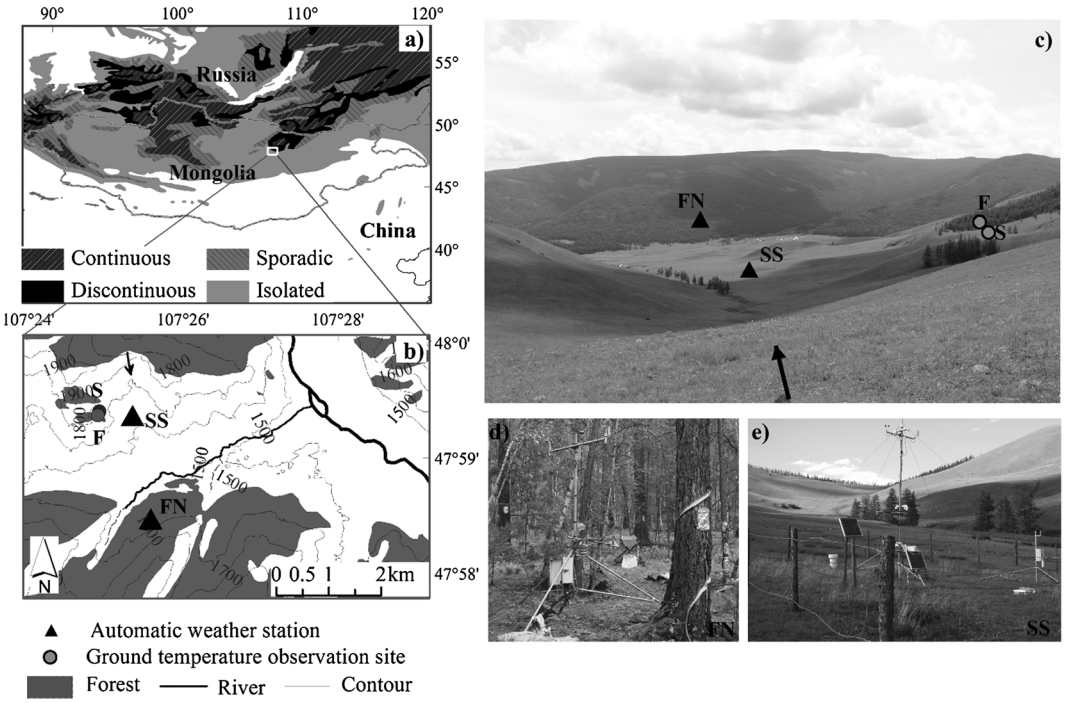

Figure 1 Location of the study area. (a) Permafrost distribution in Mongolia based on Brown *et al*. (1997). (b) Field sites FN and SS are automatic meteorological stations; F and S are shallow boreholes that contain temperature data loggers. (c) Photograph of the Shiljiree Basin showing the landscape type of each study observation site. The black arrows show the direction in which the photograph was taken. (d, e) View of the meteorological instruments at both sites.

north-facing slope (1653 m asl) covered by forest, on permafrost. Based on a vegetation survey in 2004 of both slopes, the average height and diameter at breast height of larch trees at the FN site were 16 m and 0.28 m, respectively, with a stand density of 0.15 trees m^{-2}. The dominant species were *Equisetum pretense* and *Fragaria orientalis*, and these covered approximately 50 per cent of the forest floor. At the SS site, there was a 60 per cent plant coverage consisting of *Artemisia frigida*, *Potentilla acaulis*, *Agropyron cristatum* and *Carex duriuscula*.

In addition, plots for the measurement of soil temperature at depths of 0.05 m and 1.0 m (S and F in Figure 1) were established on an east-facing slope of the study area. The plots are situated at almost the same altitude (1780 m asl), with the same orientation, inclination and vegetation cover of 60–65 per cent. Plot F is located in a small patch of forest, and plot S is in mountain steppe (only 30 m from plot F).

Data and Methods

The setup of the meteorological instruments at sites FN and SS is shown in Figure 1d and e. Air temperature at 2 m height was measured using a shielded and ventilated sensor probe (model HMP35D, Vaisala Inc., Vantaa, Finland). Downward shortwave (including direct and diffuse) radiation was measured using CM3 pyranometers (CNR-1, Kipp & Zonen, Delft, The Netherlands) with a range of 300–3000 nm at 1 m below the forest canopy at FN, and at 2 m above the steppe at SS. Soil moisture (at depths of 0.1–1.2 m) was measured using a frequency domain reflectometry sensor (EC-10, Decagon Devices, Pullman, WA, USA), and rainfall at site SS was measured using a tipping-bucket rain gauge (Rain Collector II, Davis Instruments, Hayward, CA, USA) on the ground surface. All of these measurements were sampled at intervals of 30 s (using a CR-10X data logger, Campbell Scientific Instruments, Logan, UT, USA) and were averaged and totalled every 10 min at each site. Soil temperature was measured at depths of 0, 0.1, 0.2, 0.4, 0.8, 1.0, 1.6, 2.4 and 3.25 m at site FN and at 0, 0.1, 0.2, 0.4, 0.8, 1.0, 1.6, 2.4, 3.25, 4.0 and 6.0 m at site SS using 100 ohm platinum resistance thermometers (TS101, Hakusan Kougyo, Tokyo, Japan). Soil temperature data were stored at 30 min intervals by an LS-3300 data logger (Hakusan, Tokyo, Japan). The daily average thickness of snow cover was manually measured from five fixed poles with a centimetre range at each site, and the median of these was used in the analysis.

Hydro-meteorological observations began in September 2003 and have continued to the present day. However, because of data-recording problems (e.g. instrumental failure and gaps caused by sensor malfunction, power loss, rain and frost) and missing data-sets since 2008, we only use data between 1 September 2003 and 31 December 2007. No gap filling in our data-sets was performed. We also used data obtained from the Institute of Meteorology and Hydrology of Mongolia to assess the general meteorological conditions of our study period.

Ground temperature regimes of the active layer and seasonally frozen ground were analysed using thawing/freezing degree days (TDD and FDD, respectively), the thickness of the active layer and seasonally frozen ground, the zero-curtain effect, the freezing/thawing rate and the onset of thawing/freezing. TDD was calculated as the sum of degree days above 0°C during the thawing season, and FDD as the sum of degree days below 0°C during the freezing season. Active layer thickness and seasonally frozen ground thickness were the annual maximum depth reached by the 0°C isotherm during soil thawing and freezing, respectively. Active layer thickness was determined by a linear interpolation of the soil temperature profiles between two neighbouring measurements at the time of maximum thawing (Brown *et al.*, 2000), and seasonally frozen ground thickness was estimated by maximum freezing depth. The onsets of thawing and freezing were determined by daily average ground surface temperatures that remained consistently above and below 0°C, respectively. Freezing and thawing rates describe how fast soils can freeze and thaw, and were defined by linear interpolation using the 0°C isotherm penetration based on soil temperature data. Snow thickness obtained from daily manual observations was available during the winters of 2003–04 and 2004–05, but was only collected once per month in the remaining winters. The duration of snow cover was calculated from the surface albedo, and we assumed that an albedo above 0.5 indicated the existence of snow cover.

Because we could not measure downward shortwave radiation above the forest canopy, we geometrically estimated the potential downward shortwave radiation (PDSR) above the forest canopy (site FN) and the mountain steppe (site SS) in order to clarify the downward shortwave radiation reallocation at each site. The estimation was made using the improved Advanced Spaceborne Thermal Emission and Reflection Radiometer Global Digital Elevation Model (ASTER GDEM) with a 30×30 m resolution, and the downward shortwave radiation analysis tools in ArcGIS® Spatial Analyst that calculate point and areal PDSR for any time (Huang *et al.*, 2009). The ASTER GDEM was downloaded from the Japan Space System data portal developed by the Ministry of Economy, Trade and Industry of Japan and NASA. The ASTER GDEM generally maps the top of dense land covers such as forest and urban areas (Tachikawa *et al.*, 2011), and is considered satisfactory for estimating the PDSR over the forest and steppe in our study. The simulated PDSR is the sum of direct and diffuse radiation under clear sky conditions, with consideration of topographic influences (slope, aspect, latitude and elevation) on the distribution of downward shortwave radiation (Tovar-Pescador *et al.*, 2006; Huang *et al.*, 2009). We define and use four parameters: PDSR above the forest canopy ($R_{af}\downarrow$); PDSR above the mountain steppe ($R_{as}\downarrow$); downward shortwave radiation observed below the forest canopy (1 m) at site FN ($R_{bfc}\downarrow$); and downward shortwave observed on the mountain steppe (2 m) at site SS ($R_s\downarrow$). With no forest cover at site SS, the coefficient of cloud cover (k_c) for a given time was calculated as 1 minus

the ratio of downward shortwave radiation at the surface ($R_s\downarrow$) to the downward shortwave over the mountain steppe $R_{as}\downarrow$:

$$k_c = 1 - (R_s\downarrow/R_{as}\downarrow). \quad (1)$$

We consider that values of k_c at SS and FN are almost the same, because the cloud frequencies at the two adjacent sites are almost identical. Thus, we estimated the downward shortwave radiation above the forest canopy ($R_{afc}\downarrow$) for site FN as:

$$R_{afc}\downarrow = (R_{af}\downarrow - R_{af}\downarrow * k_c). \quad (2)$$

We estimated the coefficient of forest cover as:

$$k_f = 1 - (R_{bfc}\downarrow / R_{afc}\downarrow). \quad (3)$$

The magnitudes of the coefficients of cloud cover and forest range from 0 to 1, and can be indicated by a percentage.

RESULTS

General Meteorological Conditions

The automatic soil weather stations at the sites indicated a climate characterised by low precipitation and large annual variations in air temperature (Table 1). The warmest year of the study period was 2007, with a mean annual air temperature (MAAT) of -1.7°C (resulting primarily from a dry hot summer), and the coldest year was 2006, with a MAAT of -3.3°C at the FN site. The maximum and minimum daily air temperatures ranged from 27.4°C to -34.2°C at SS, and from 24.2°C to -36.3°C at FN. The snow-free periods observed at FN in 2005 and 2006 were longer than those of other years. Total precipitation from April to September during the study period ranged from 223 mm in 2007 to 295 mm in 2005.

Ulaanbaatar station (UB) is one of the nearest permanent meteorological stations, located 40 km west of the study site, where the long-term mean (1980–2010) air temperature was -0.3°C. In the study period, the MAAT at UB was 0.4, 0.3, -0.3 and 1.9°C in 2004, 2005, 2006 and 2007, respectively. Therefore, it is inferred that those MAATs over the study period were generally higher than the long-term mean temperature at UB. Annual precipitation at UB ranged from 166 mm to 395 mm (mean annual precipitation from 1980–2010 was 265 mm), of which approximately 90 per cent occurred between April and September. The mean annual total precipitation at UB was 260, 193, 256 and 185 mm in 2004, 2005, 2006 and 2007, respectively. This indicates that the study period was dry.

Hydro-meteorological Variables

Figure 2 shows the annual cycles of daily downward shortwave radiation on the steppe and below the forest canopy, and the air and surface temperatures at sites SS and FN. The annual variations in downward shortwave radiation at both sites were markedly affected by solar elevation, vegetation cover and weather conditions.

During summer, the SS site received more downward shortwave radiation than the FN site, with peaks of 411 Wm^{-2} and 403 Wm^{-2} at the end of June 2006 and June 2007, respectively, at the SS site. At the FN site, the amount of downward shortwave radiation below the forest canopy strongly related to the canopy density. Peak values of downward shortwave radiation below the forest canopy ranged from 126.9 Wm^{-2} to 155.2 Wm^{-2}, and typically occurred at the end of May, approximately 1 month earlier than at site SS. Thereafter, at the beginning of the leaf-growing period, downward shortwave radiation below the forest canopy began to decrease steadily between June and the end of September, the onset of leaf senescence. It increased slightly for a few days during mid-September (Figure 2a), and this was attributed to initial leaf loss from the forest canopy.

In winter, downward shortwave radiation is low and remains almost stable at each site due to the lower solar angles. The lowest downward shortwave radiation value (nearly 0) below the forest canopy at FN occurred between mid-December and the beginning of January. The average downward shortwave radiation from December to February was 95, 96.8, 108.5 and 92.3 Wm^{-2} at SS and 10.5, 8.7, 11.3 and 10.1 Wm^{-2} below the forest canopy at FN in the winters of 2003–04, 2004–05, 2005–06 and 2006–07, respectively (Figure 2a).

Although similar patterns in daily air temperature were measured at both FN and SS, air temperatures at FN were

Table 1 General meteorological parameters at the mountain steppe south-facing slope (site SS) and the forested north-facing slope (site FN).

Variable	Units	Site	2004	2005	2006	2007
Maximum air temperature	°C	SS/FN	23.3/22.6	na/21.7	21.1/17.8	27.4/24.2
Minimum air temperature	°C	SS/FN	−28.4/-29.1	−30.2/-30.8	−34.2/-36.3	−23.9/-26.5
Mean annual air temperature	°C	SS/FN	na/-2.1	na/-2.9	na/-3.3	na/-1.7
Rainfall (Apr–Sep)	mm	SS	243	295	227	223
Duration of snow-free period	days	SS/FN	232/194	268/214	na/202	249/185

na = Non-available data in all tables.

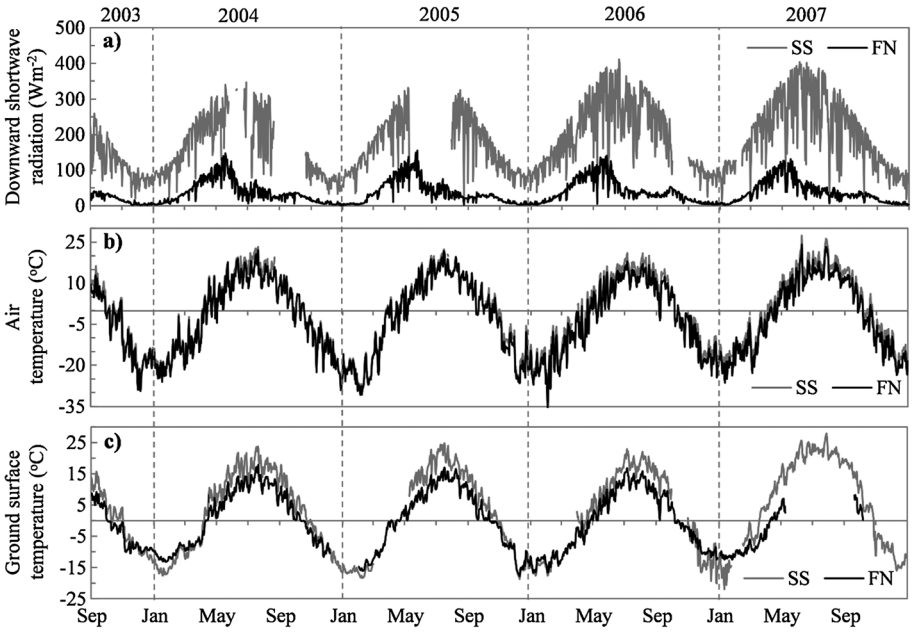

Figure 2 Daily average (a) downward shortwave radiation (below the forest canopy at 1 m and on the mountain steppe at 2 m); (b) air temperature; and (c) ground surface temperature from 1 September 2003 to the end of 2007 measured at the mountain steppe south-facing slope (SS) and the forested north-facing slope (FN).

lower than those at SS during summer and winter (Figure 2b). The differences in air temperatures between the two sites from May to August for the summers of 2004, 2006 and 2007 were 2.0, 2.6 and 2.7°C, respectively. However, the air temperature differences between the two sites from November to February were lower, at 0.9, 0.6 and 2°C during the first three winters, respectively.

At SS, the surface temperature in summer exceeded the air temperature, and the opposite occurred at FN (Table 2). In addition, year-round surface temperature fluctuations were higher at SS than at FN, and the former site was considerably warmer in summer and slightly colder in winter than the latter (Figure 2c). These seasonal differences in ground surface temperatures between the two sites can be mostly explained by interannual variations in downward shortwave radiation at the ground surface, together with variations in snow cover and soil moisture content. The near-surface soil moisture at SS (0.1–0.2 m depth) seldom exceeded 20 per cent after rainfall, and immediately started to decrease until the following rainfall (Figure 3b). Only small seasonal variations in soil moisture occurred in deeper layers (0.4, 0.8 and 1.2 m) and the values of soil moisture did not exceed 12 per cent during the study period (Figure 3b), indicating that soil at the SS site is dry. It is therefore likely that the higher downward shortwave radiation on the dry ground at SS causes a warm soil profile during summer compared to the profile at FN. For example, the mean summer ground surface temperature (May–August) at SS was warmer by 5.4°C in 2004 and 5.5°C in 2006 than at FN, respectively (Table 2). Such differences in ground surface temperatures between the sites were also evident in other summers (2005 and 2007); however, no complete temperature data were available for this period (Figure 2c).

Interannual variations in snow cover showed similar patterns at both sites (Figure 4), although the thickness and duration of snow cover were greater at FN than at SS. Owing to the thicker snow cover, the surface temperature during winter was higher at FN than at SS, despite the lower air temperature at FN (Table 3). The air temperature in

Table 2 Summer air and ground surface temperatures at the mountain steppe south-facing slope (SS) and the forested north-facing slope (FN).

Variable	Units	Site	2004	2005	2006	2007
Mean air temperature (May–Aug)	°C	SS/FN	13.6/11.6	na/11.4	11.7/9.1	15.4/12.7
Mean surface temperature (May–Aug)	°C	SS/FN	15.6/10.2	na/9.5	14.5/9	20/na
TDD_{air}	°Cdays	SS/FN	na/1753	na/1726	na/1495	2356/1866
TDD_{sur}	°Cdays	SS/FN	2495/1522	na/1436	na/1409	3453/na

TDD_{air} = Thawing degree days of air; TDD_{sur} = Thawing degree days of surface.

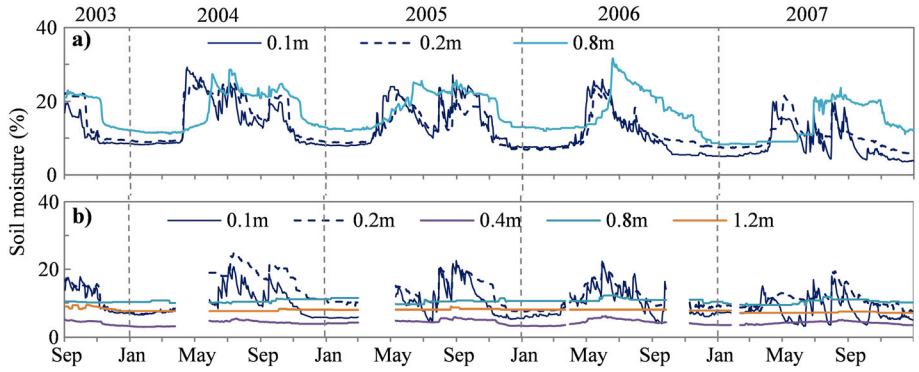

Figure 3 Soil moisture content from 1 September 2003 to the end of 2007 measured at (a) the forested north-facing slope; and (b) the mountain steppe south-facing slope. This figure is available in colour online at wileyonlinelibrary.com/journal/ppp

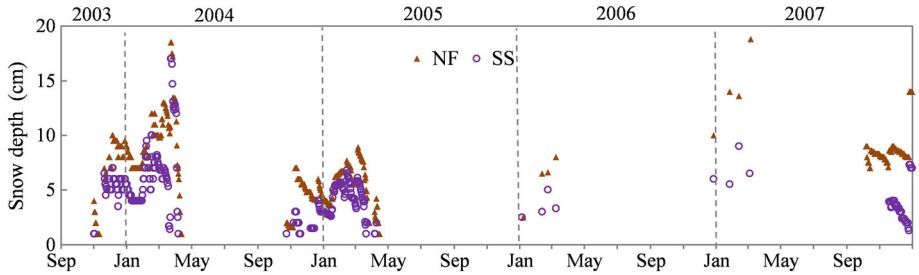

Figure 4 Thickness of snow cover on the mountain steppe south-facing slope (SS) and the forested north-facing slope (FN), measured during the winters of the study period. This figure is available in colour online at wileyonlinelibrary.com/journal/ppp

Table 3 Winter air and ground surface temperatures, snow thickness and duration, and thickness of seasonally frozen ground at the study sites: the mountain steppe south-facing slope (site SS) and the forested north-facing slope (site FN).

Variable	Units	Site	2003–04	2004–05	2005–06	2006–07
Mean air temperature (Nov–Feb)	°C	SS/FN	-17.9/-18.8	-16.9/-17.5	-15.8/-17.8	na/-16.5
Mean surface temperature (Nov–Feb)	°C	SS/FN	-11/-9.7	-11.4/na	-11.8/-11.6	na/-9.4
FDD_{sur}	°Cdays	SS/FN	-1635/-1504	na/na	na/-1789	na/-1427
Duration of snow cover	day	SS/FN	141/159	114/162	85/140	111/170
Maximum snow thickness	cm	SS/FN	17/18.6	6.8/8.9	5/8	10/17.5
Seasonal frozen ground thickness	m	SS	3.9	4	4.4	3.7

FDD_{sur} = Freezing degree days of surface.

winter was lower than the surface temperature at both sites. As summarised in Table 3, the snow cover effect is seen clearly in the interannual variations in ground surface temperatures at each site. For example, during the cold winter of 2003–04, when average air temperatures from November–February were -17.9°C at SS and -18.8°C at FN, the maximum thickness and duration of snow cover were 17 cm and 141 days at SS and 18.6 cm and 159 days at FN, which resulted in large differences in the seasonal evolution of air and surface temperatures at each site. In contrast, during the winter of 2005–06, when average air temperatures were -15.8°C at SS and -17.8°C at FN, there was a reduced maximum thickness and duration of snow cover at SS (5 cm and 85 days) and FN (8 cm and 140 days). As a result, differences in the seasonal evolution of air and surface temperatures at each site were small. Furthermore, despite the cold winter in 2003–04, both the ground surface temperature and freezing degree days of surface at two sites were greater than in the winter of 2005–06.

Dynamics of the Active Layer and Seasonal Frozen Ground

Figure 5 shows interannual variations in soil temperature at FN, from the surface to a depth of 3.2 m. The active layer usually begins to thaw at the end of April, with an average

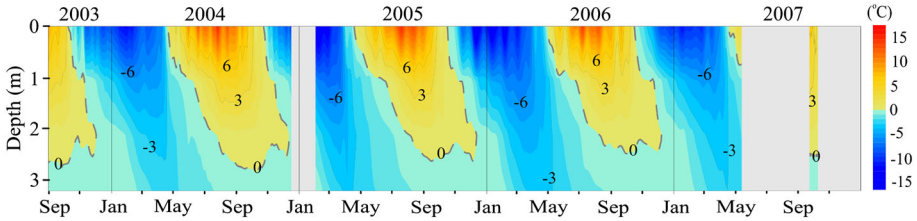

Figure 5 Seasonal changes in daily average soil temperature between 0 m and 3.2 m depths for the whole observation period at the forested north-facing slope (FN). 1°C isotherm interval. The grey or open areas indicate missing data. This figure is available in colour online at wileyonlinelibrary.com/journal/ppp

thawing ratio of 0.022 m day^{-1} from the surface to a depth of 2 m (the average from the first three summers). The maximum active layer thickness was usually observed in mid-September, and was strongly related to thawing degree days of air (TDD_{air}) for FN (Table 2). In 2004–06, the active layer thickness peaked at 2.67 m in 2004 (the year in which the higher TDD_{air} occurred), and in the summers of 2005 and 2006 was 2.6 m and 2.4 m, respectively (at a time when TDD_{air} was moderately low). However, the hottest summer occurred in 2007, when TDD_{air} was 1866°C days, during which time the active layer thickness developed to more than 2.5 m in early September (thereafter further developing) (Figure 5). Such results indicate that air temperature during summer is the dominant factor controlling the thickness of the active layer.

Refreezing of the active layer usually begins in mid-October, and it is completely frozen by the end of December. The depth of penetration of soil refreezing is inhibited by the latent heat of fusion (Hinkel *et al.*, 2001), and during some of this period soil temperatures remain close to 0°C; this is known as the zero-curtain effect (Outcalt *et al.*, 1990). Soils at site FN contain abundant water, particularly in the deeper soil layers (Figure 3a), and as a result, a longer freezing zero-curtain effect was observed at a depth of 1 m for a duration of 20, 27 and 34 days in 2004, 2005 and 2006, respectively. Despite the zero-curtain effect and the thicker snow accumulation at this site compared to that at SS, soil freezing penetrated rapidly, at 0.043 m day^{-1} between the ground surface and a depth of 2 m during all the recorded winters.

As shown in Figure 6, seasonally frozen ground at SS began to thaw in early April immediately after the disappearance of snow cover, and the thawing deepened quickly, at rates of 0.057 m day^{-1} and 0.054 m day^{-1} to a depth of 2 m in 2004 and 2006, respectively (twice as fast as the rates at site FN). The ground had thawed completely by 30 June in 2004 and 17 June in 2005, but not until 18 August in 2006 (Figure 6).

Thermal insulation from snow cover was a more important factor in controlling the development of seasonally frozen ground thickness than air temperature. The seasonally frozen ground thickness at SS was 3.9 m in 2003–04 and 4.4 m in 2005–06, even though air temperature was lower during the former winter than during the latter (Table 3). By examining subsequent records, we found that the thickness and duration of snow cover decreased from 2003–04 to 2005–06 and the seasonally frozen ground thickness increased (Figures 4 and 6; Table 3). However, this situation was reversed in the winter of 2006–07: the increased thickness (10 cm) and duration (111 days) of snow cover resulted in a decreased seasonally frozen ground thickness of 3.7 m. This demonstrates that thin snow cover with a shorter duration potentially leads to deeper seasonal freezing of ground.

Comparison of Ground Temperature in Forested and Steppe Areas

Given that the F and S plots are located in the same geographical area and that their soils are practically identical (mostly sand and gravel) (Ishikawa *et al.*, 2005), the main differences in the ground surface temperature between the plots likely reflect differences in vegetation cover (forest and steppe). As shown in Figure 7a, plot S is colder than plot F during winter, but warmer in summer. The average surface temperatures from June to September in the summer of 2004 were 10.8°C at F and 16.7°C at S, and 10.4°C and

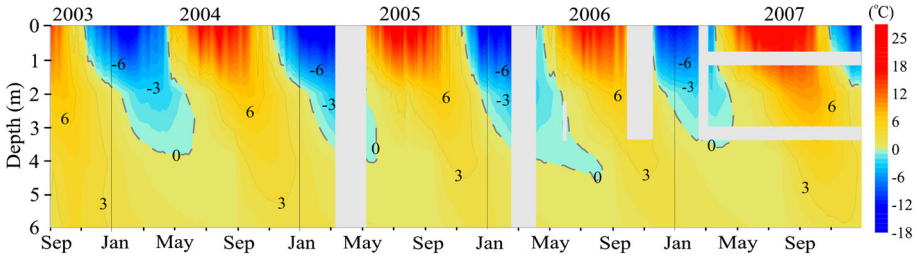

Figure 6 Seasonal changes in daily average soil temperatures between 0 m and 6 m depths for the whole observation period at the mountain steppe on the south-facing slope (SS). 1°C isotherm interval. The grey or open areas indicate missing data. This figure is available in colour online at wileyonlinelibrary.com/journal/ppp

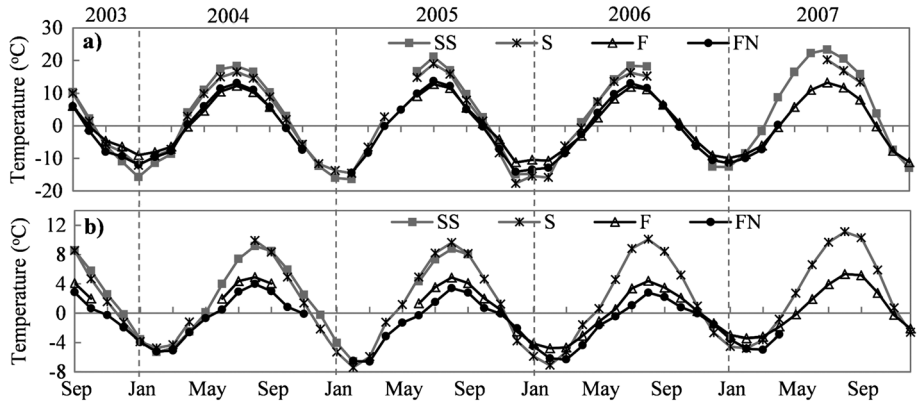

Figure 7 Monthly patterns in soil temperature from 1 September 2003 to the end of 2007 at all observation sites: (a) surface temperatures; and (b) soil temperatures at 1 m depth.

15°C, respectively, in the summer of 2006. In contrast, in winter, the difference in surface temperature between these sites was small owing to snow insulation, and depended strongly on the interannual variation in snow accumulation. In the winter of 2003–04, the snow cover was thick and the surface temperature averaged from November to March was -8.7°C at F and -8.9°C at S. However, for the same period during the winter of 2005–06, there was only a thin snow cover, and the averaged surface temperatures were -11.4°C at F and -12.6°C at S.

The effects of vegetation cover and the soil organic layer on ground temperature are also shown in Figure 7. The ground surface temperatures measured at sites F and FN were similar during all summers (Figure 7a), which suggests that the low temperature on the forest floor is usually related to forest cover and not to site location or soil composition. For the steppe areas, site SS showed a slightly higher surface temperature in summer than site S (Figure 7a), and this variance is explained partly by the differences in slope, aspect and elevation. Figure 7b suggests that the organic layer strongly influenced ground temperature at greater depth. Despite similar ground surface temperatures at F and FN in summer, the ground temperatures at 1 m showed large variations; the monthly ground temperature at F was 1.3–2.3°C higher in the summers of 2004, 2005 and 2006 than that at FN, and this is attributed to differences in the soil organic layer. According to Ishikawa *et al*. (2005), the thickness of the organic layer at site F was 0.1 m which is twice as thin as those along the north-facing slope, where site FN is located. However, the observed differences of monthly ground temperature at 1 m between sites F and FN ranged from 0.1°C to 1.4°C during the winters of 2005–06 and 2006–07. These results indicate that the dominant thermal insulator affecting ground surface temperature within the mosaic throughout the year was mainly vegetation cover rather than snow cover. A thick organic layer on forested slopes favours the existence of permafrost.

Table 4 shows the onset of thawing and freezing during the observation period. The onset of thawing at the ground surface occurred earlier in the steppe sites than in the forest sites. For example, in 2004 and 2006 the onset of thawing was noted on days of the year 98 and 109 at site S, respectively, which is 9 and 13 days earlier, respectively, than at the adjacent forested area F. Likewise, the onset of thawing at site S at a depth of 1 m was several days earlier than at site F. In contrast, the onset of freezing occurred approximately on the same day at both sites (Table 4).

Table 4 Dates of onset of spring thawing and autumn freezing for plots F and S from 2004 to the end of 2006.

Year	Depth (cm)	F		S	
		O_t	O_f	O_t	O_f
2004	0	107	294	98	295
	100	146	na	123	334
2005	0	na	289	98	289
	100	na	329	128	329
2006	0	122	290	109	na
	100	162	325	134	326

O_t and O_f represent the day of the year when the onset of thawing and freezing occurred, respectively.

Solar Radiation Allocation on Both Slope Types

Downward shortwave radiation reaching the ground surface has a major effect on net radiation. We describe here the effects of the forest canopy and topography on the downward shortwave radiation redistribution at SS and FN, using GDEM data and measured downward shortwave radiation data. The monthly PDSR ($R_{af}\downarrow$ and $R_{as}\downarrow$) has higher values than the monthly measured downward shortwave radiation ($R_{bfc}\downarrow$ and $R_s\downarrow$) at both sites, owing to effects such as clouds, aerosols and precipitation (Figure 8). However, the monthly variations in $R_s\downarrow$ correspond closely with those of $R_{as}\downarrow$ ($R^2 = 0.96$, $p < 0.0001$) throughout the year, but monthly variations in $R_{af}\downarrow$ and $R_{bfc}\downarrow$ show very different patterns in their development ($R^2 = 0.52$, $p < 0.04$), mainly

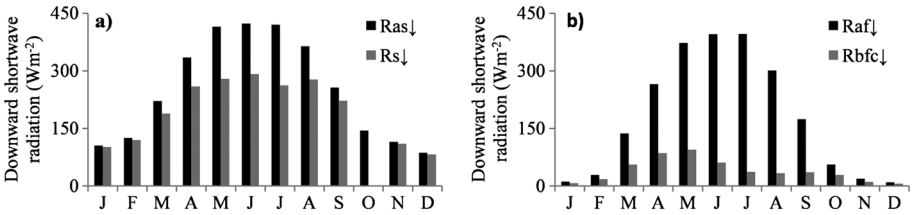

Figure 8 Monthly average simulated ($R_{af}\downarrow$ = above the forest canopy, $R_{as}\downarrow$ = above the mountain steppe) and observed downward shortwave radiation ($R_{bfc}\downarrow$ = below the forest canopy, $R_s\downarrow$ = on the mountain steppe) for 2006 at (a) the mountain steppe south-facing slope; and (b) the forested north-facing slope.

Table 5 Coefficients of cloud cover over the study area (k_c) and forest cover (k_f) at the forested north-facing slope (FN), and monthly downward shortwave radiation ($R_{afc}\downarrow$) (Wm^{-2}) over the forest at FN for 2006.

	Jan	Feb	Mar	Apr	May	Jun	Jul	Aug	Sep	Oct	Nov	Dec
k_c	0.03	0.04	0.15	0.23	0.33	0.31	0.38	0.24	0.13	na	0.04	0.04
k_f	0.33	0.34	0.52	0.58	0.62	0.78	0.85	0.86	0.77	na	0.39	0.37
$R_{afc}\downarrow$	11.1	27.1	116.8	205.1	251.1	272.6	247.0	229.5	151.2	na	18.2	9.4

due to the evolution of the forest canopy. The monthly differences between $R_{as}\downarrow$ and $R_{af}\downarrow$ may represent a topographical effect on downward shortwave radiation. These differences ranged from 76.2 Wm^{-2} to 97.3 Wm^{-2} during winter, but between only 28 Wm^{-2} and 24.3 Wm^{-2} in June and July, when the position of the sun (zenith and azimuth angles) reduced the difference between them. It is therefore evident that the effect of topography on downward shortwave radiation is higher in winter than in summer on the north-facing slope, and this is probably one of the factors delaying the period of snow settling on the north-facing slope compared to the south-facing slope (Figure 4; Table 3).

In our study area, small values of k_c (0.03–0.15) during winter might be related to the clear skies over Mongolia, caused by strong anticyclones (Zhang *et al*., 2008). In contrast, large values of k_c (0.13–0.38) were observed in summer (Table 5), when most of the yearly precipitation falls in Mongolia. The shelter effect of the forest canopy on monthly downward shortwave radiation was assessed by the data presented in Table 5. From January to August, k_f values increased and then decreased until December. These changes are associated with the life cycle of forest leaves. During the full-leaf period, particularly in June, July and August, k_f was higher (0.78–0.86), owing to the strong shading provided by the forest canopy. This means that only 22–14 per cent of downward shortwave radiation over the forest reaches the forest floor, and that 78–86 per cent is sheltered by the forest canopy. In winter, k_f was lower (0.33–0.37 between December and February). These results suggest that downward shortwave radiation reaching the forest floor is affected not only by forest leaf evolution in summer, but also by bare trees in winter.

$R_{bfc}\downarrow$ generally showed small values, but values of $R_{afc}\downarrow$ (Table 5) and $R_s\downarrow$ on steppe were distinctly higher than those in subarctic and Arctic zones during summer (see Eugster *et al*., 2000). These results show that the considerable differences in observed downward shortwave radiation between the two sites were caused mostly by forest cover. Hence, the reduced downward shortwave radiation on the ground within the forested area is likely to limit the heat exchange between the ground and the atmosphere.

DISCUSSION

Our results exhibit that the interannual variations in soil temperatures under the forest floor differ significantly from those of the adjacent mountain steppe, and that the air and ground temperatures in the forest are colder. These differences are mainly associated with the behaviour of the local climate, vegetation cover and thermal properties of the ground.

Mountain Steppe

As shown in Figure 4, the disappearance of snow cover occurred several days earlier at site SS than at site FN in spring, implying that the available heat storage on the surface could be used efficiently in soil heating and turbulent heat fluxes, thereby substantially lengthening the thawing season. As almost all summer precipitation was consumed by evapotranspiration at SS (Iijima *et al*., 2012), soils were generally dry there during summer (Figure 3b). Therefore, more downward shortwave radiation on the dry ground surface at SS probably caused a warm soil profile in summer. The soil texture beneath the south-facing slope is characterised by sandy gravel (Ishikawa *et al*., 2005), which has a higher thermal conductivity (Williams and Smith, 1989) than the gravelly soil with a deeper organic layer on the north-facing slope. Less soil moisture in the ground facilitates soil freezing and thawing, because less

energy is required for a phase change into soil water, and this is confirmed by the lack of zero-curtain effects that were observed within the soil upper layer during the entire observation period. These combined effects are thought to drive rapid soil warming at the SS site during summer, resulting in rapid thawing of seasonally frozen ground.

Snow cover is one of the most important factors determining ground temperature variations during winter because it limits heat exchanges between the ground and the atmosphere owing to its low heat conductivity (Williams and Smith, 1989; Zhang, 2005). The thinner snow cover at SS than at FN and the shorter retention period (Figure 4; Table 3) are attributed mainly to the greater sublimation and wind scour. Zhang *et al*. (2008) reported sublimation from snow cover at SS as $0.16\,\mathrm{mm\,day^{-1}}$, which is twice as high as that at FN. Thus, there is a smaller effect from snow insulation in the steppe areas, releasing more heat from dry ground to the atmosphere, thereby enabling deep seasonal freezing at SS.

Forested Slope

The strong reduction in the amount of downward shortwave radiation on the forest floor (Figure 2) is related to its modulation by the evolution of forest canopy and the slope, and is one of the factors that reduced ground surface temperatures in summer in the forested areas compared to the steppe (Figure 7a). The seasonal evolution of the forest canopy in north central Mongolia has been illustrated in other studies (Iijima *et al*., 2012; Miyazaki *et al*., 2014), where it has been observed that leaves emerge in May, mature in July and die in mid-September. Permafrost beneath forested north-facing slopes is impermeable to groundwater flow (Ishikawa *et al*., 2005), and it reduces evapotranspiration from this slope (Iijima *et al*., 2012). This results in wet ground at FN (Figure 3a), which generally has a higher thermal conductivity than dry soils (Farouki, 1981; Hinzman *et al*., 1991) and should therefore contribute to heat transfer from the ground surface to deep soil layers, enabling a warm soil profile. However, soil temperatures in the deeper layers at FN are generally colder than at other sites during summer (Figure 7b), probably indicating that the thick organic layer at the site has an efficient impact on keeping the ground cool, because of the low thermal conductivity of organic layer under the unfrozen state (Williams and Smith, 1989). The cooling effect of thick organic layers during summer has been reported in other boreal forested regions in Alaska and Kamchatka (Yoshikawa *et al*., 2003; Fukui *et al*., 2008). In addition, the longer-lasting snow cover at the forested site (FN) shortens the summer thawing period. Therefore, these combined effects at FN retard summer warming, and reduce soil temperatures during summer compared with those at site SS.

As shown in Figure 2c and Table 3, the insulation effect of low-conductivity snow cover on the ground surface temperature is more significant at FN than at SS in winter, although the thick organic layer at site FN probably contributes to ground heat loss due to its high thermal conductivity in the frozen state (Williams and Smith, 1989). The ice content of the upper ground layer at FN during winter was probably considerably higher than that at site SS, as the soil moisture values were higher during autumn. The ice content within the upper frozen soil would also promote rapid heat transfer, due to its high thermal conductivity and low heat capacity. Thus, the ground temperature fell rapidly, which leads to quick refreezing of the active layer at FN.

For comparison, a study within the forest-tundra ecotone of North America shows that the heterogeneity of the ground temperature within the ecotone is controlled by the snow-holding capacity of local vegetation patches and the spatial configuration of land covers, and that the ground temperature generally decreases across the treeline, from the taiga to landscapes dominated by low shrubs and sedges (Roy-Léveillée *et al*., 2014). Additionally, overall, the onset of thawing was earlier, but the onset of freezing in our study area was later than those in evergreen conifer, larch and tundra at high northern latitudes (Smith *et al*., 2004).

CONCLUSIONS

The following conclusions are drawn from this study:

1. In summer, the ground surface temperature is considerably warmer at the steppe site SS than at the forest site FN, probably because of the large amount of downward shortwave radiation received on the dry south-facing slope (site SS), which results in rapid thawing of seasonally frozen ground and a warm soil profile. Conversely, the forest canopy on the north-facing slope (site FN) significantly reduces air temperature and the amount of downward shortwave radiation reaching the ground, thereby causing an air temperature that is higher than the surface temperature. In addition, the thick soil organic layer strongly limits heat transfer to the deeper soil layers.
2. In winter, the surface temperature is warmer on the forested slopes than on the steppe slopes, owing to the thicker snow cover on the former. However, the thick organic layer beneath the snow cover enhances the freezing rate, especially at FN. The snow cover duration and thickness at SS are inversely related to the thickness of seasonally frozen ground.
3. Differences in downward shortwave radiation and ground surface temperatures between the forest and steppe sites in summer largely result from the presence of forest canopy, which prevents 33–86 per cent of the total amount of downward shortwave radiation above it from reaching the forest floor throughout the year.
4. Forested areas and the underlying thick organic layer at the edge of the Siberian boreal forest are both important factors contributing to the existence of permafrost in this region, which occurs only beneath forested north-facing slopes.

ACKNOWLEDGEMENTS

We would like to thank the Editor, Julian Murton, and two anonymous reviewers for their valuable suggestions and constructive comments. This study was supported by the Frontier Observational Research System for Global Change and the Research Institute for Global Change, Japan Agency for Marine-Earth Science and Technology, the Ministry of Education, Science, Sports and Culture of Japan and by the State Education Fund from the Ministry of Education and Science, Mongolia. We thank all participants who helped during the fieldwork and operation of the weather stations at each study site.

REFERENCES

Batima P. 2006. Climate Change Vulnerability and Adaption in the Livestock Sector of Mongolia. Final Report, Project No. AS06. Assessments of Impacts and Adaption to Climate Change: Washington, DC.

Batima P, Dagvadorj D. 2000. Climate change and its impacts in Mongolia. National Agency for Meteorology, Hydrology and Environment Monitoring and JEMR Publishing: Ulaanbaatar.

Brown J, Ferrians OJ, Jr, Heginbottom JA, Melnikov ES. 1997. Circum-Arctic Map of Permafrost and Ground-Ice Conditions. Circum-Pacific Map Series CP-45, scale 1: 10,000,000, 1 sheet. US Geological Survey in Cooperation with the Circum-Pacific Council for Energy and Mineral Resources: US Geological Survey in Cooperation with the Circum-Pacific Council for Energy and Mineral Resources.

Brown J, Hinkel KM, Nelson FE. 2000. The Circumpolar Active Layer Monitoring (CALM) Program: Research designs and initial results. *Polar Geography* **24**(3): 165–258.

Dulamsuren C, Hauck M, Leuschner HH, Leuschner C. 2011. Climate response of tree-ring with in Larinx Sibirica growing in the drought-stressed forest-steppe ecotone of northern Mongolia. *Annals of Forest Science* **68**: 275–282. DOI: 10.1007/s13595-011-0043-9

Etzelmüller B, Heggem ESF, Sharkhuu N, Frauenfelder R, Kääb A, Goulden C. 2006. Mountain permafrost distribution modeling using a multi-criteria approach in the Hövsgöl Area, Northern Mongolia. *Permafrost and Periglacial Processes* **17**: 91–104. DOI: 10.1002/ppp.554

Eugster W, Rouse RW, Pielke RA, Sr, McFadden JP, Baldocchi DD, Kittel TGF, Chapin FS, III, Liston GE, Vidale PL, Vaganov E, Chambers S. 2000. Land–atmosphere energy exchange in Arctic tundra and boreal forest: available data and feedbacks to climate. *Global Change Biology* **6**: 84–115. DOI: 10.1046/j.1365-2486.2000.06015.x

Farouki OT. 1981. Thermal properties of soils. CRREL Monograph 81-1, U.S. Army Corps of Engineers Cold Regions Research and Engineering Laboratory: Hanover, New Hampshire, USA.

Frauenfeld OW, Zhang T. 2011. An observational 71-year history of seasonally frozen ground changes in the Eurasian high latitudes. *Environmental Research Letters* **6**: 044024. DOI: 10.1088/1748-9326/6/4/044024

Frauenfeld OW, Zhang T, Barry RG, Gilichinsky D. 2004. Interdecadal changes in seasonal freeze and thaw depths in Russia. *Journal of Geophysical Research* **109**: D05101. DOI: 10.1029/2003JD004245

Fukui K, Sone T, Yamagata K, Otsuki Y, Sawada Y, Vetrova V, Vyatkina M. 2008. Relationships between permafrost distribution and surface organic layers near Esso, central Kamchatka, Russian Far East. *Permafrost and Periglacial Processes* **19**: 85–92. DOI: 10.1002/ppp.606

Heggem ESF, Etzelmüller B, Anarmaa S, Sharkhuu N, Goulden CE, Nadintsetseg B. 2006. Spatial distribution of ground surface temperatures and active layer depths in the Hovsgol Area, Northern Mongolia. *Permafrost and Periglacial Processes* **17**: 357–369. DOI: 10.1002/ppp568

Hinkel KM, Paetzold F, Nelson FE, Bocheim JG. 2001. Patterns of soil temperature and moisture in the active layer and upper permafrost at Barrow, Alaska: 1993-1999. *Global and Planetary Change* **29**: 293–309.

Hinzman LD, Kane DL, Gleck RE, Everett KR. 1991. Hydrological and thermal properties of the active layer in the Alaskan Arctic. *Cold Region Science and Technology* **19**: 95–110.

Huang S, NASA Ames Researcher Center, Fu P, ESRI. 2009. Modeling Small Areas Is a Big Challenge Using the Solar Radiation Analysis Tools in ArcGIS Spatial Analyst, ArcUser. http://www.esri.com

Iijima Y, Fedorov AN, Park H, Suzuki K, Yabuki H, Maximov TC, Ohata T. 2010. Abrupt increases in soil temperatures following increased precipitation in a permafrost region, central Lena river basin, Russia. *Permafrost and Periglacial Processes* **21**: 30–41. DOI: 10.1002/ppp.662

Iijima Y, Ishikawa M, Jambaljav Y. 2012. Hydrological cycle in relation to permafrost environment in forest-grassland ecotone in Mongolia. *Journal of Japanese Association of Hydrological Sciences* **42**: 119–130 (in Japanese with English abstract).

Ishikawa M, Sharkhuu N, Zhang Y, Kadota T, Ohata T. 2005. Ground thermal and moisture conditions at the southern boundary of discontinuous permafrost, Mongolia. *Permafrost and Periglacial Processes* **16**: 209–216. DOI: 10.1002/ppp483

Ishikawa M, Zhang Y, Kadota T, Ohata T. 2006. Hydrothermal regimes of the dry active layer. *Water Resources Research* **42**(4): W04401. DOI: 10.1029/2005WR004200

Ishikawa M, Iijima Y, Zhang Y, Kadota T, Yabuki H, Ohata T, Battogtokh D, Sharkhuu N. 2008. Comparable energy balance measurements on the permafrost and immediate adjacent permafrost-free slopes at the southern boundary of Eurasian permafrost, Mongolia. In Permafrost, Proceeding of the Ninth International Conference on Permafrost, Vol. **1**. University of Alaska Fairbanks, 29 June–3 July 2008, Kane DL, Hinkel KM (eds). Institute of Northern Engineering, University of Alaska: Fairbanks, Alaska; 795–800.

Ishikawa M, Sharkhuu N, Jambaljav Y, Davaa D, Yoshikawa K, Ohata T. 2012. Thermal state of Mongolian permafrost. In Proceedings of the Tenth International Conference on Permafrost, Vol. **1**. 25–29 June, Salekhard, Yamal-Nenets Autonomous District, Russia, Hinkel KM (eds.). The Northern Publisher: Salekhard, Russia; 173–178.

Miyazaki S, Ishikawa M, Baatarbileg N, Damdinsuren S, Ariuntuya N, Jambaljav Y. 2014. Interannual and seasonal variations in energy and carbon exchanges over the larch forests on the permafrost in northeastern Mongolia. *Polar Science*. DOI: 10.1016/j.polar.2013.12.004

Outcalt SI, Nelson FE, Hinkel KM. 1990. The zero curtain effect: Heat and mass transfer across an isothermal region in freezing soil. *Water Resources Research* **26**(7): 1509–1516. DOI: 10.1029/WR026i007p01509

Roy-Léveillée P, Burn CR, McDonald DI. 2014. Vegetation-permafrost relations within the forest-tundra ecotone near Old Crow, Northern Yukon, Canada. *Permafrost and Periglacial Processes* **25**: 127–135. DOI: 10.1002/ppp1805

Sharkhuu A, Sharkhuu N, Etzelmüller B, Heggem ESF, Nelson FE, Shiklomanov NI, Goulden CE, Brown J. 2007. Permafrost monitoring in the Hovsgol mountain region, Mongolia. *Journal of Geophysical Research* **112**: F02S06. DOI: 10.1029/2006JF000543

Shiklomanov NI, Streletskiy DA, Nelson FE, Hollister RD, Romanovsky VE, Tweedie CE, Bockheim JG, Brown J. 2010. Decadal variations of active-layer thickness in moisture-controlled landscapes, Barrow, Alaska. *Journal of Geophysical Research – Biogeosciences* **115**: G00I04. DOI: 10.1029/2009JG001248

Smith VN, Saatchi SS, Randerson TJ. 2004. Trends in high northern latitude soil freeze and thaw cycles from 1988 to 2000. *Journal of Geophysical Research – Atmospheres* **109**: D12101. DOI: 10.1029/2003DJ004472

Sugita M, Asanuma J, Tsujimura M, Mariko S, Lu M, Kimura F, Azzaya D, Adyasuren T. 2007. An overview of the rangelands atmosphere-hydroshere-biosphere interation study experiment in northeastern Asia (RAISE). *Journal of Hydrology* **333**: 3–20. DOI: 10.1016/j.jhydrol.2006.07.032

Tachikawa T, Kaku M, Iwasaki A, Gesch D, Oimoen M, Zhang Z, Danielson J, Krieger T, Curtis B, Haase J, Abrams M, Crippen R, Carabajal C. 2011. ASTER Global Digital Elevation Model Version 2 – Summary of Validation Results by the ASTER GDEM Validation Team, August 31, 2011. https://www.jspacesystems.or.jp/ersdac/GDEM/ver2Validation/Summary_GDEM2_validation_report_final.pdf

Tovar-Pescador J, Pozo-Vázquez D, Ruiz-Arias JA, Batlles J, López G, Bosh JL. 2006. On the use of the digital elevation model to estimate the solar radiation in areas of complex topography. *Meteorological Applications* **13**: 279–287. DOI: 10.1017/S1350482706002258

Tsogtbaatar J. 2004. Deforestation and reforestations needs in Mongolia. *Forest Ecology and Management* **201**(1): 57–63.

Walker DA, Jia GJ, Epstein HE, Raynolds MK, Chapin FS, III, Copass C, Hinzman LD, Knudson JA, Maier HA, Michaelson GJ, Nelson F, Ping CL, Romanovsky VE, Shiklomanov N. 2003. Vegetation-soil-thaw-depth relationships along a Low-Artic bio-climate gradient, Alaska: Synthesis of information from the ATLAS studies. *Permafrost and Periglacial Processes* **14**(2): 103–123. DOI: 10.1002/ppp.452

Williams P, Smith M. 1989. The Frozen Earth: Fundamentals of Geocryology. Cambridge University Press: Cambridge.

Wu Q, Zhang T. 2010. Changes in active layer thickness over the Qinghai-Tibetan Plateau from 1995 to 2007. *Journal of Geophysical Research – Atmospheres* **115**: D09107. DOI: 10.29/2009JD012974

Wu T, Zhao L, Li R, Xie Ch, Pang Q, Wang Q, Batkhishig O, Battogtokh B. 2012. Permafrost degradation under abrupt warming in the Central Mongolia Plateau. In Proceedings of the Tenth International Conference on Permafrost, Vol. **4**. 25–29 June, Salekhard, Yamal-Nenets Autonomous District, Russia, Drozdov DS (ed). The Northern Publisher: Salekhard, Russia; 589–590.

Yoshikawa K, Bolton WR, Romanovsky VE, Fukuda M, Hinzman LD. 2003. Impacts of wildfire on the permafrost in the boreal forests of Interior Alaska. *Journal of Geophysical Research* **108**: D1 8148. DOI: 10.1029/2001JD000438

Zhang T. 2005. Influence of the seasonal snow cover on the ground thermal regime: an overview. *Reviews of Geophysics* **43**: RG4002. DOI: 10.1029/2004RG000157

Zhang T, Frauenfeld OW, Serreze MC, Etringer A, Oelke C, McCreight J, Barry RG, Gilichinsky D, Yang D, Ye H, Ling F, Chudinova S. 2005. Spatial and temporal variability in active layer thickness over the Russian Arctic drainage basin. *Journal of Geophysical Research – Atmospheres* **110**: D16101. DOI: 10.1029/2004JD005642

Zhang Y, Ishikawa M, Ohata T, Oyunbaatar D. 2008. Sublimation from thin snow cover at the edge of the Eurasian cryosphere in Mongolia. *Hydrological Processes* **22**: 3564–3575. DOI: 10.1002/hyp.6960

Zhao L, Wu Q, Marchenko SS, Sharkhuu N. 2010. Thermal state of permafrost and active layer in central Asia during the international polar year. *Permafrost and Periglacial Processes* **21**: 198–207. DOI: 10.1002/ppp688

